The Plant Journal (2006) **45**, 1017–1027 doi: 10.1111/j.1365-313X.2006.02663.x

The *Agrobacterium vitis* T-6b oncoprotein induces auxin-independent cell expansion in tobacco

Bernadette Clément[1], Stephan Pollmann[2], Elmar Weiler[2], Ewa Urbanczyk-Wochniak[3] and Léon Otten[1,*]
[1]*Department of Cell Biology, Institut de Biologie Moléculaire des Plantes, Rue du Général Zimmer 12, 67084 Strasbourg, France,*
[2]*Lehrstuhl für Pflanzenphysiologie, Ruhr-Universität Bochum, Universitätsstrasse 150, ND3/55, 44801 Bochum, Germany, and*
[3]*Max-Planck-Institut für Molekulare Pflanzenphysiologie, Am Mühlenberg 1, 14476 Golm, Germany*

Received 30 September 2005; revised 21 November 2005; accepted 25 November 2005.
*For correspondence (fax +33 388614442; e-mail leon.otten@ibmp-ulp.u-strasbg.fr).

Summary

Among the *Agrobacterium* T-DNA genes, *rolB*, *rolC*, *orf13*, *orf8*, *lso*, *6b* and several other genes encode weakly homologous proteins with remarkable effects on plant growth. The *6b* oncogene induces tumors and enations. In order to study its properties we have used transgenic tobacco plants that carry a dexamethasone-inducible *6b* gene, dex-T-*6b*. Upon induction, dex-T-*6b* plants develop a large array of morphological modifications, some of which involve abnormal cell expansion. In the present investigation, dex-T-*6b*-induced expansion was studied in intact leaves and an *in vitro* leaf disc system. Although T-*6b* and indole-3-acetic acid (IAA) both induced expansion and were non-additive, T-*6b* expression did not increase IAA levels, nor did it induce an IAA-responsive gene. Fusicoccin (FC) is known to stimulate expansion by increasing cell wall plasticity. T-*6b*- and FC-induced expansion were additive at saturating FC concentrations, indicating that T-*6b* does not act by a similar mechanism to FC. T-*6b* expression led to higher leaf osmolality values, in contrast to FC, suggesting that the T-*6b* gene induces expansion by increasing osmolyte concentrations. Metabolite profiling showed that glucose and fructose played a major role in this increase. We infer that T-*6b* disrupts the osmoregulatory controls that govern cell expansion during development and wound healing.

Keywords: *Agrobacterium*, metabolite profiling, oncogenes, osmolytes, *plast* family, tumors.

Introduction

The *Agrobacterium plast* gene family defined by Levesque *et al.* (1988) on the basis of weak protein homologies includes T-DNA genes such as *rolB*, *rolC*, *orf13*, *6a*, *6b*, *lso* and *Norf8* [for reviews on these genes see Nilsson and Olsson (1997) and Meyer *et al.* (2000); for a recent protein alignment see Helfer *et al.* (2002)]. Each of these genes induces highly specific growth modifications, but little is known about their modes of action. So far they have only been found in *Agrobacterium* T-DNAs and in some plant species; the latter are considered to result from ancient *Agrobacterium* transformation events (Meyer *et al.*, 2000). A retinoblastoma-binding motif (LxCxE) has been found in the ORF13 protein (Stieger *et al.*, 2004) but not in 46 other RolB-like proteins (Helfer *et al.*, 2002). Likewise, a tyrosine phosphatase motif (CX_5R) found in A4-RolB (Filippini *et al.*, 1996) has not been found in other RolB or RolB-like proteins. A glucosidase-like activity has been reported for RolB (Estruch *et al.*, 1991b) and RolC (Estruch *et al.*, 1991a), defining the RolB/RolC glucosidase family (PF02027) of the Pfam database (Bateman *et al.*, 2004), but this enzymatic function has been put into doubt by subsequent experiments (reviewed in Nilsson and Olsson, 1997).

The developmental and physiological changes that lead to the various *plast* gene-induced phenotypes have been little studied. Among the *plast* genes, *6b* genes have remarkable and unique effects on plant growth. They induce tumors on certain hosts (Hooykaas *et al.*, 1988; Tinland *et al.*, 1989) and dramatic morphological changes in transgenic tobacco plants that express AB-*6b* (from *Agrobacterium* strain AB4), T-*6b* (Tm4) or AK-*6b* (AKE-10) (Grémillon *et al.*, 2004; Helfer *et al.*, 2003; Tinland *et al.*, 1992; Wabiko and Minemura, 1996). They develop enations, catacorollas, tubular leaves, expanded cotyledons, corkscrew stems, short thick roots, ectopic shoots on hypocotyls, fragmented leaf primordia,

vein thickening, hyponastic petioles and epinastic leaf veins. We have called this remarkable and unique set of *6b*-induced modifications the enation syndrome (Helfer *et al.*, 2003). The syndrome results from two distinct effects: local *6b* expression and movement of one or more non-identified *6b*-induced enation factors (EF). The EF traffics through the phloem, crosses graft junctions and especially affects the growth of young tissues (Grémillon *et al.*, 2004; Helfer *et al.*, 2003). Although we earlier found that T-*6b*-transformed *N. rustica* hypocotyl fragments could not transmit their *6b* phenotype to grafted wild-type hypocotyls (Tinland *et al.*, 1992), this was probably due to the lack of a vascular connection between the fragments (Otten, unpublished data).

Gene *6b*-induced growth modifications have been compared to phytohormone effects. Spanier *et al.* (1989) noted that *6b* reduced cytokinin sensitivity. Cytokinin measurements with AK-*6b*-transformed tobacco plants showed no modification of cytokinin levels (Gális *et al.*, 1999; Wabiko and Minemura, 1996). Bonnard *et al.* (1989) reported that, whereas agrobacteria carrying a cytokinin synthesis gene (*ipt*) induced shoots on tobacco stems, mixed infections with agrobacteria carrying *ipt* and *6b* genes induced undifferentiated tumors as did a combination of *ipt* and *iaa* (auxin synthesis) genes, suggesting that the growth-modifying effects of *6b* genes may result from an increase in auxin levels. However, *6b*-carrying agrobacteria could not replace exogenous auxins in an auxin-dependent *rolABC*-based rooting assay (Tinland *et al.*, 1990), indicating that they do not increase auxin levels or auxin sensitivity. Moreover, *6b*-expressing plants do not have typical auxin phenotypes (Grémillon *et al.*, 2004; Helfer *et al.*, 2003; Tinland *et al.*, 1992), although they show enhanced cell expansion and epinastic growth, both of which are auxin-like effects. Therefore, it remains possible that *6b* genes induce only part of the auxin response repertoire or that their activity requires additional factors.

Recent work showed that the AK-6b protein is localized in the nucleus and that its nuclear transport depends on a transcription factor-like plant protein, NtSIP1 (Kitakura *et al.*, 2002). Fluctuations in NtSIP1 concentrations might restrict *6b*-induced effects. In tobacco, C58-*6b* gene expression is accompanied by increased indole-3-acetic acid (IAA) levels; this was attributed to an accumulation of flavonoids that might protect IAA against degradation and thus induce growth changes (Gális *et al.*, 2002). However, the IAA increase in these plants could be a secondary effect resulting from severe growth changes due to *6b* expression during development. To assess the possible role of auxins in *6b*-induced growth modifications, we used dexamethasone (dex)-inducible dex-T-*6b* tobacco plants (Grémillon *et al.*, 2004) and an IAA-sensitive leaf disc expansion assay (Keller and Van Volkenburgh, 1997). Although dex-T-*6b* induction stimulated expansion, endogenous IAA concentrations and the expression of IAA-induced genes remained unaffected, showing that T-*6b*-induced leaf expansion does not act through an increase in IAA. Additional experiments provided new insight into the mechanism by which T-*6b* expression influences plant growth.

Results

T-6b *gene induction stimulates leaf disc expansion*

Plants of dex-T-*6b* tobacco transgenics are morphologically normal and do not produce detectable T-6b amounts without induction (Grémillon *et al.*, 2004). T-6b protein synthesis in the homozygous one-copy line D6Nt17 could be induced in expanding leaves (at about 80% of their final size) by infiltration with 20 μM dex, the first signals on Western blots being visible at 6 h (Figure 1a). The first enation factor effects were observed on young non-infiltrated leaves situated above the infiltrated leaves, 3–4 days after induction. Leaves up to 7 cm (at the time of infiltration) curled downwards along the entire rim, whereas older leaves (7–15 cm) only curled at the base (Figure 1b). Leaves also showed epinastic bending of mid-veins and hyponastic bending of petioles (Figure 1c). Artificially introduced holes in dex-infiltrated patches showed cell hypertrophy at the rims (Figure 1d), and needle holes showed chlorosis and expansion (Figure 1e) about one week after induction. At later stages, dex-infiltrated areas developed chlorosis that subsequently extended to the entire surface of the infiltrated leaf half (Figure 1f). In order to study leaf expansion in more detail, we used an *in vitro* leaf disc expansion assay that has been developed for *Nicotiana tabacum* cv. Xanthi (Keller and Van Volkenburgh, 1997, 1998). As the D6Nt17 line was derived from cv. Samsun nn (Grémillon *et al.*, 2004), the growth of which differs considerably from that of cv. Xanthi, we first characterized the expansion properties of non-induced D6Nt17 discs. Because the capacity for expansion *in vitro* depends on leaf age (Keller and Van Volkenburgh, 1997), we systematically analyzed discs of several succeeding leaves, in order to obtain a more reliable picture of changes induced by the different treatments. On M90 medium, discs expanded regularly for over 6 days with a fresh weight (FW) increase of 15–40% per day, with younger leaves showing more expansion (Figure 2a).

We next tested the influence of sucrose on disc expansion by varying its concentration from 0–90 mM while keeping medium osmolality at 110 mOsm by adding the non-permeant osmolyte sorbitol. Maximal expansion was obtained at 72 mM sucrose for three different leaf sizes (Figure 2b). Subsequently, all experiments were performed with M60 medium without sorbitol.

The effect of dex-T-*6b* expression on expansion was measured by floating D6Nt17 leaf discs on M60 with different dex concentrations. No disc curvature was

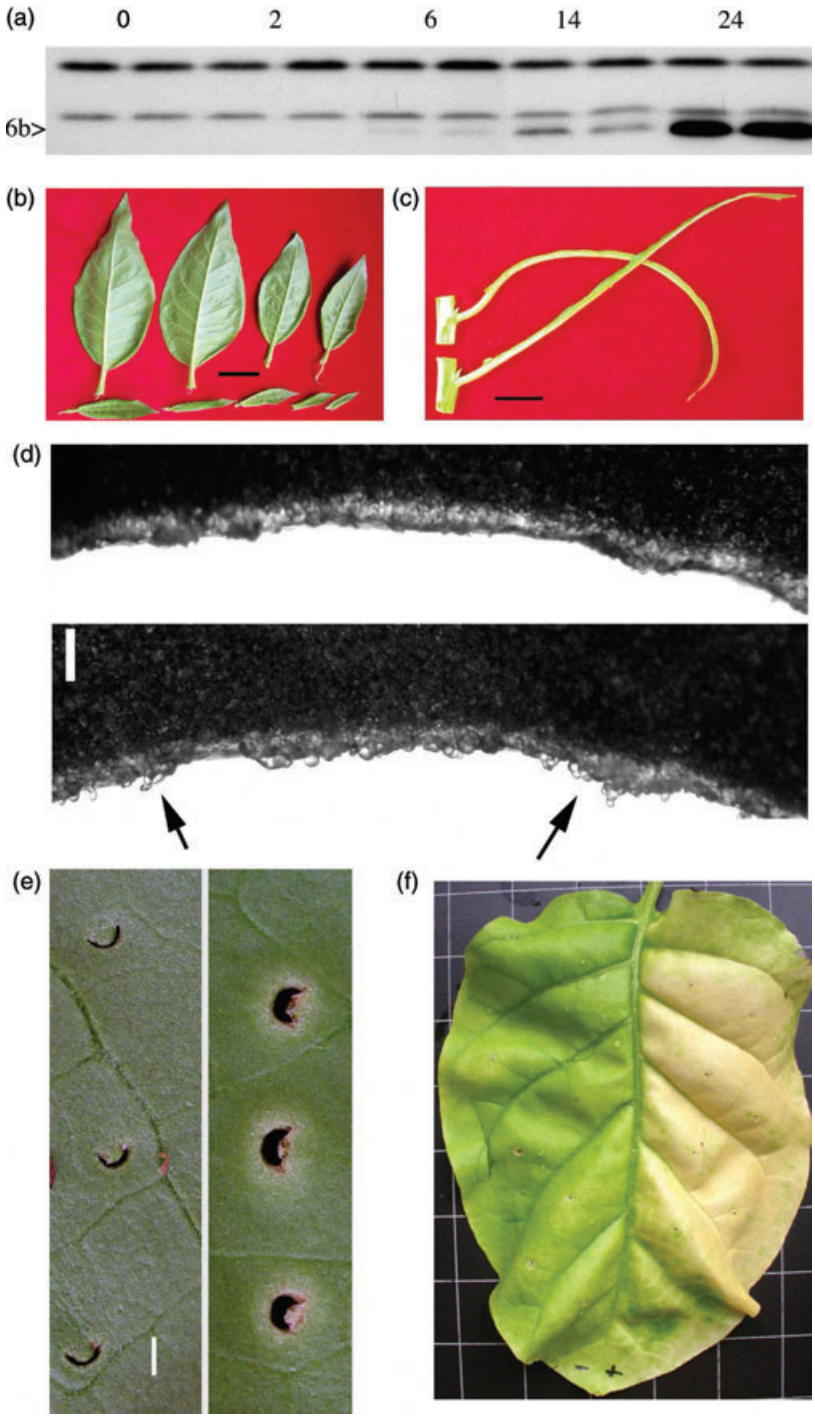

Figure 1. Effects of infiltration of D6Nt17 (dex-T-*6b*) leaves with dexamethasone.
(a) Induction of T-6b protein as shown by Western analysis; duplicate samples taken 0, 2, 6, 14 and 24 h after infiltration of D6Nt17 leaves with 20 μM dex. The T-6b protein (arrow) becomes detectable from 6 h onwards; the two other bands are non-specific.
(b) Epinastic curling of the leaf rims of 9 young, non-induced leaves above a dex-induced leaf. Size bar, 2 cm. Upper row, leaves 1–4; lower row, leaves 5–9.
(c) Epinastic bending of a midrib of a non-induced leaf (leaf blade removed) above a dex-induced leaf. The petiole shows hyponastic bending. Size bar, 4 cm. Petiole and midrib from a control leaf above a mock-induced leaf show no bending.
(d) Cell expansion on the rim of a circular hole (1 cm diameter) within a mock-induced patch (upper part) and dex-induced patch (lower part). Arrows indicate hypertrophic cells. Size bar, 0.5 mm.
(e) Differences between wound reactions in a mock-induced patch (left, no reaction) and dex-induced patch (right, expansion and chlorosis). Patches were wounded with a needle of 1 mm diameter. Size bar, 1 mm.
(f) Leaf chlorosis 3 weeks after induction. The left half of the leaf was mock-induced, the right half dex-induced. Only the induced half shows chlorosis. Size marker of background grid, 3 cm.

observed. The observed FW changes might be partly due to cell division. In cultivar Samsun nn, the expression of cell division-associated genes sharply declines after leaves have reached a length of 5 cm (Helfer *et al.*, 2003), i.e. well below the size of the leaves used for the present experiments. In the case of *6b*-controlled cell division, these genes should again be induced. We therefore measured the expression of *CaKN* (knolle), *NtPCNA* (proliferating cell nuclear antigen) and *NtCYC1* (cyclin) genes (Helfer *et al.*, 2003) as probes, in mock-induced and in dex-induced discs (24 h after induction). RNA of young leaves (3–4 cm length) was used as a positive control. Hybridization to the actin gene *NtACT1* (CAA45149.1) was used as an RNA loading control. Whereas the cell cycle genes were highly expressed in young leaves,

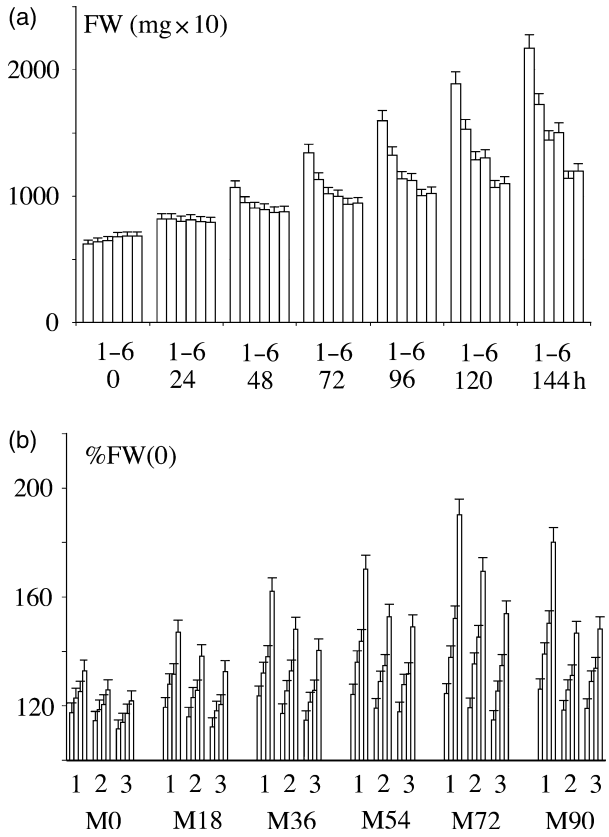

Figure 2. Expansion of non-induced D6Nt17 leaf discs *in vitro*.
(a) Expansion of discs from successive leaves with lengths of 8, 9, 11.5, 12.5, 14 and 15 cm (1–6). Discs were floated on M90. Fresh weights increase regularly over a period of 144 h.
(b) Influence of sucrose concentration on expansion. Three successive leaves (1–3, lengths of 18.5, 24 and 25 cm) were tested. Discs were floated on medium with 0, 18, 36, 54, 72 and 90 mM sucrose complemented with sorbitol to a medium osmolality of 110 mOsm. Fresh weights were measured at 16, 29, 40 and 90 h and expressed as percentage of initial FW. Maximal growth occurs in M72 (72 mM sucrose).

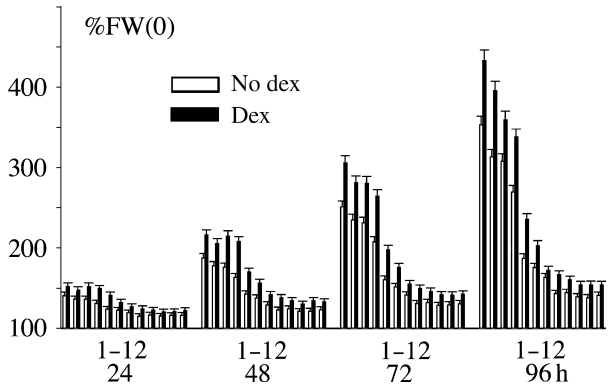

Figure 3. Effects of dex induction on expansion of D6Nt17 discs *in vitro*.
Discs of twelve successive D6Nt17 leaves with lengths of 9, 13, 15, 17, 21.5, 25, 26, 25.5, 24, 25.5, 23 and 24 cm (1–12) were floated on M60 (white bars) or M60 + 3 μM dex (black bars). Fresh weights increased over a period of 96 h. Dex-treated discs expand faster than control discs.

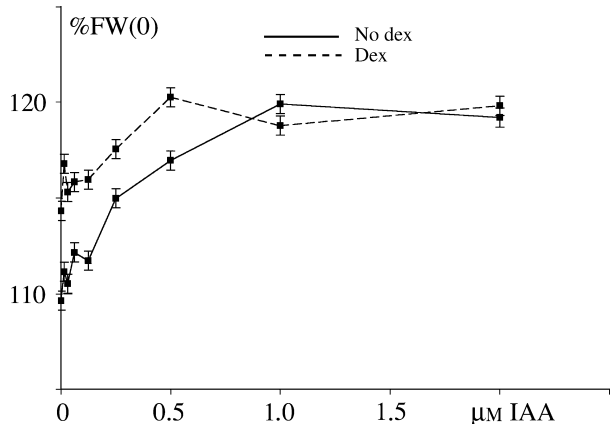

Figure 4. Expansion of D6Nt17 leaf discs in M60 with different indole-3-acetic acid (IAA) concentrations in the absence (continuous lines) or presence (discontinuous lines) of 3 μM dex.
Indole-3-acetic acid and T-6b expansion values are not additive.

no expression could be detected in mock-induced or dex-induced discs (<0.1% for *NtPCNA*, <1% for *CaKN* and *NtCYC1*, results not shown). As we found a 16% volume increase in dex-treated discs compared to control discs, whereas *NtPCNA* expression levels only allowed a maximum of 0.1% of cell division, we conclude that the FW increase was mainly due to cell expansion. M60 with 3 μM dex (called M60D) was used for all further induction experiments. Dex-T-*6b* expression led to an increase in expansion within a large range of leaf sizes (from 9–26 cm length; Figure 3).

6b-*induced leaf disc expansion is not transmitted to untransformed discs*

We have shown previously that *6b*-expressing plants can induce strong enation growth effects in grafted non-transformed tissues (Grémillon *et al.*, 2004; Helfer *et al.*, 2003), suggesting that *6b*-expressing tissues produce a mobile growth factor. In mixed cultures of wild-type leaf discs and dex-induced D6Nt17 discs (at a proportion of one wild-type disc for 50 D6Nt17 discs), we observed <0.3% additional expansion of wild-type discs compared to similar mixtures in the absence of dex. Thus, no mobile factor could be demonstrated in the leaf disc assay.

*Comparison between auxin-induced and T-*6b*-induced expansion*

Auxin leads to expansion and epinastic curvature of leaf explants (Keller and Van Volkenburgh, 1997). D6Nt17 leaf discs were floated on M60 with different IAA concentrations, without dex. Leaf curling occurred from 1.0–2.0 μM IAA onwards. Expansion increased from 0.1 to 1.0 μM IAA

Table 1 Indole-3-acetic acid concentrations in mock-induced and dex-induced D6Nt17 leaf discs, different times after infiltration

Time (h)	No dex [pmol indole-3-acetic acid (IAA) g^{-1} fresh weight (FW)] (mean, $n = 10$)	SD (pmol IAA g^{-1} FW)	Dex (pmol IAA g^{-1} FW) (mean, $n = 10$)	SD (pmol IAA g^{-1} FW)
0	24.1	7.6	20.3	5.8
3	15.0	4.9	13.2	2.9
6	16.3	3.2	16.5	7.4
9	17.5	9.9	13.9	4.1
12	19.4	12.4	20.2	11.2

None of the differences are significant as determined by Student's *t*-test ($P < 0.05$).

Table 2 Expression levels of the *NtIAA2.3/2.5* gene after different treatments of leaf discs for 24 h, measured by Northern analysis

Control ($n = 3$)	SD	+Dex ($n = 3$)	SD	+IAA ($n = 3$)	SD	IAA + dex ($n = 3$)	SD
28.2	2.8	27.0	6.0	117.9	2.8	122.3	7.6

Hybridization signals at different film exposure times were measured by ImageJ analysis, expressed in arbitrary units and normalized to actin expression levels. Control, M60 medium; dex, 3 μM dex in M60; IAA, 0.1 μM IAA in M60. Differences between control and dex treatments on the one hand, and between IAA and IAA + dex treatments on the other hand, are not statistically significant (as determined by Student's *t*-test, $P < 0.05$).

(Figure 4a). On M60D with 3 μM dex, without IAA, expansion reached the same values as on 0.1–0.2 μM IAA. At saturating IAA concentrations (1–2 μM), dex addition did not lead to further expansion (Figure 4a). This suggests that *6b* and IAA act in a similar way, and is in accordance with the hypothesis that *6b* acts by increasing IAA levels (Gális *et al.*, 2002). We therefore measured IAA levels in D6Nt17 discs on M60 or M60D at 3 h intervals over a period of 12 h. Under both conditions, IAA levels remained constant (as analyzed by Student's *t*-test, $P < 0.05$), within a range of 13–25 pmol g^{-1} FW (Table 1). We subsequently used the auxin-responsive gene *Nt-IAA2.3/2.5* (or *AK3.2*; Dargeviciute *et al.*, 1998) as an indicator for changes in IAA concentration. In order to exclude the possibility that T-*6b* expression would repress IAA-mediated *Nt-IAA2.3/2.5* induction, thereby masking a possible increase in IAA, discs were treated with 3 μM dex and a sub-optimal IAA concentration of 0.1 μM. In the absence of IAA, T-*6b* expression did not significantly increase *Nt-IAA2.3/2.5* transcript levels. In the presence of 0.1 μM IAA, it did not modify the induction of *Nt-IAA2.3/2.5* (as determined by Student's *t*-test, $P < 0.05$) (Table 2). We therefore conclude that T-*6b* induction does not modify IAA levels.

T-6b- *and fusicoccin-induced expansion are additive*

The fungal phytotoxin fusicoccin (FC) increases cell wall plasticity by activating the plasma membrane H^+-ATPase through interaction with a 14-3-3 protein (Aducci *et al.*, 1995; Würtele *et al.*, 2003). The resulting acidification weakens the cell wall, and leads to expansion if osmolyte concentrations are sufficiently high. In order to test whether T-*6b*-induced expansion results from a similar effect, we compared FC- and T-*6b*-induced disc expansion in M60 medium. FC strongly induced the expansion of D6Nt17 leaf discs or wild-type tobacco discs, as already reported for cv. Xanthi (Keller and Van Volkenburgh, 1997). Expansion was maximal at 0.7–1.0 μM FC (not shown). The expansion induced by dex (medium M60D) was equivalent to the expansion induced by 0.15 μM FC (medium FC-0.15) for four different leaf sizes, as analyzed by two-factor analysis of variance (Figure 5a). FC- and T-*6b*-induced expansions were additive even at the saturating FC concentration of 1 μM (Figure 5b), suggesting that T-*6b*-induced expansion does not result from cell wall acidification. We reasoned that if T-*6b* was still able to enhance expansion at maximal FC concentration, it might do so by increasing osmolyte concentrations. Whereas treatment with FC led to a decrease in osmolality (as expected on the basis of osmolyte dilution during expansion, at least before osmotic compensation sets in), T-*6b* induction caused an increase (Figure 5c). A similar increase also occurred in dex-infiltrated D6Nt17 leaves *in situ* (Figure 5d). These findings strongly suggest that T-*6b*-induced expansion results from changes in osmolyte concentrations.

T-6b *increases glucose and fructose concentrations*

Expression of the *6b*-related *plast* gene *Norf8* leads to high levels of soluble sugars and starch in tobacco leaves (Otten and Helfer, 2001; Umber *et al.*, 2002, 2005). Starch accumulation was also observed in 2x35S-AB-*6b* (Helfer *et al.*, 2003) and induced dex-T-*6b* plants (Grémillon *et al.*, 2004; this paper). We therefore tested whether the T-*6b*-induced osmolality increase involved soluble sugars. After 24 h of induction, intact dex-infiltrated D6Nt17 leaves contained significantly more glucose, fructose and sucrose than mock-infiltrated leaves. Glucose and fructose increased in parallel by a factor of 3–4, whereas sucrose levels increased by a factor of 2–3 (Figure 6a). In discs cultured on M60 medium

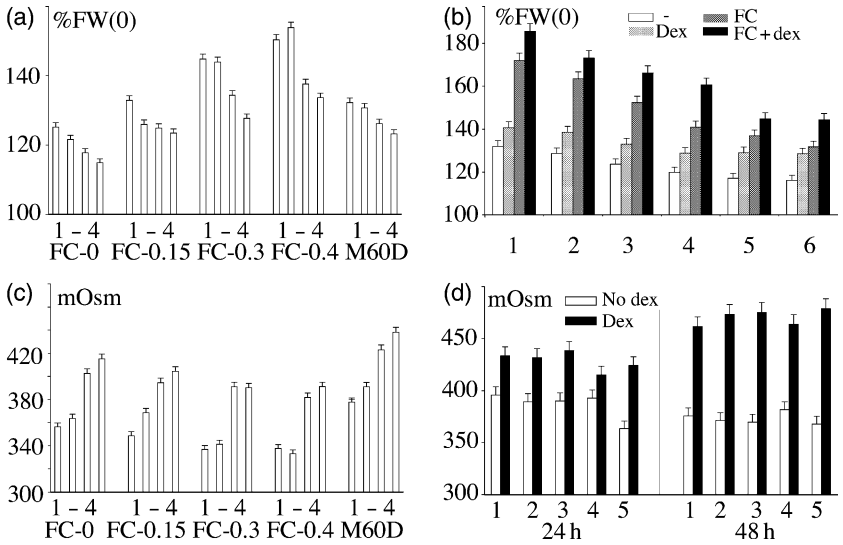

Figure 5. Expansion and osmolality of D6Nt17 discs in M60 medium with fusicoccin (FC) or 3 μM dex (M60D).
(a) Discs of four successive leaves (1–4, lengths of 20.5, 22.5, 25.0 and 27.0 cm) were incubated for 24 h on M60 with different FC concentrations (0, 0.15, 0.3 and 0.4 μM) or on M60D. T-6b induced expansion on M60D is similar to the expansion induced by 0.15 μM FC. (b) Discs from six successive D6Nt17 leaves (1–6, lengths of 13.5, 16.7, 18.0, 19.0, 20.3 and 20 cm) were floated on M60 (white bars), M60D (light grey bars), M60 + 1 μM FC (dark grey bars) or M60D + 1 μM FC (black bars). Fresh weights were measured 24 h later. Expansions induced by T-6b and FC are additive. (c) Osmolality of the same samples as in (a). Osmolality decreases with increasing FC concentration. The osmolalities of the M60D samples are higher than the osmolalities of untreated samples, and, most notably, of the FC-0.15 samples that undergo similar levels of expansion as M60D. (d) Osmolality in mock-induced (white bars) and dex-induced (black bars) D6Nt17 leaves. Patch positions on the leaves are numbered 1–5 (apical to basal). Measurements after 24 and 48 h. Osmolalities are higher in T-6b-expressing leaves.

we expected a gradient due to uptake and metabolism of sucrose from the medium. We therefore analyzed the rims and central parts of the discs separately. As expected, the rims contained more glucose, fructose and sucrose than the central parts after 24 h of incubation. On M60D, glucose and fructose levels were higher than on M60, both at the rims and in the central parts, while sucrose levels were not notably modified (Figure 6b).

The conspicuously parallel increase in glucose and fructose in dex-induced leaves and leaf discs suggested an increase in invertase activity. However, the activities of the three types of invertases (cytosolic, vacuolar and cell wall invertases) in induced leaves remained very similar to those of control leaves (Figure 7).

The increase in glucose and fructose concentrations in dex-induced leaves (about 15–30 mM) might significantly contribute to the overall increase in leaf sap osmolality (about 40 mOsm). However, amino acids, organic acids and potassium ions (Stiles *et al.*, 2003) could also play a role. We therefore measured a large range of metabolites by a metabolite profiling approach and also determined potassium values in dex-infiltrated D6Nt17 leaves and control leaves.

Metabolite profiling and potassium analysis of induced and non-induced leaves

Metabolite profiling provides a qualitative and quantitative view of the major metabolites in different plant tissues. Induced and non-induced D6Nt17 leaves were analyzed for metabolites according to the method described by Roessner-Tunali *et al.* (2003). The results (Table 3) show that the levels of several metabolites significantly increased. Glutamine, proline, glucose and fructose increased more than threefold, ascorbate and putrescine between two- and threefold. When these data are scrutinized, it becomes clear that the primary metabolites that can contribute to the osmotic potential of the cell and are the building blocks for the polymers required for growth are elevated in the cell, whereas the secondary metabolites were generally unchanged. Glucose and fructose contribute most to the overall increase. Potassium levels were very similar in dex-treated and control tissues, both in intact leaves *in situ* and in discs *in vitro* (Figure 8), showing that potassium plays no osmotic role in T-*6b*-induced leaf expansion.

Discussion

Morphogenetic effects of *6b* gene expression are pleiotropic and not easily reducible to a known type of aberrant growth, either induced by hormones or by mutation, with the possible exception of some uncharacterized tobacco mutants that form catacorollas, or the unexplored growth effects of enation viruses (Grémillon *et al.*, 2004; Helfer *et al.*, 2003). In spite of this, we postulate that a single molecular mechanism will eventually explain each aspect of the enation syndrome. The data presented here suggest that stimulation of cell expansion during normal and

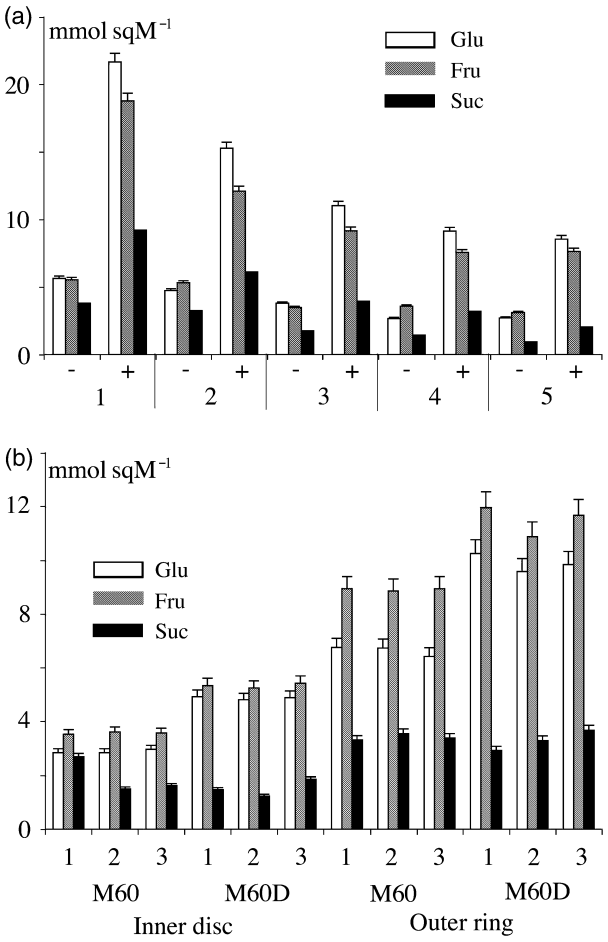

Figure 6. Increase in soluble sugars in dex-infiltrated D6Nt17 leaves.
(a) Increase in glucose, fructose and sucrose concentrations in patches of five successive mock-infiltrated (–) or dex-infiltrated (+) D6Nt17 leaves (1–5, lengths of 16, 25, 25, 22.5, 17.5 and 13.5 cm) after 24 h of induction.
(b) Increase in glucose, fructose and sucrose concentrations in leaf discs of 1.6 cm diameter floated on M60 and M60D, from three successive leaves (1–3, lengths of 22, 24, 25.5 cm). After 24 h incubation, each disc was divided into two parts: an inner disc of 1.0 cm diameter and the remaining outer ring. The inner parts of non-induced discs contain less soluble sugars than the outer parts. T-6b induction leads to an increase in glucose and fructose concentrations in both parts. White bars, glucose; grey bars, fructose; black bars, sucrose.

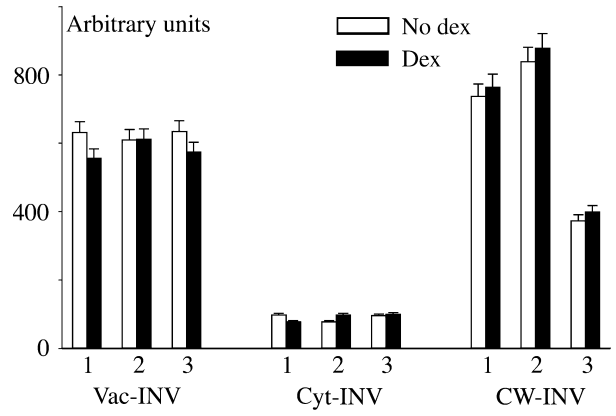

Figure 7. Invertase activities in mock-infiltrated (white bars) and dex-infiltrated (black bars) D6Nt17 leaves.
Three successive leaves (1–3, lengths of 24, 25, 26.5 cm) were used. T-6b induction does not lead to a significant increase in vacuolar invertase (vac-INV), cytosolic invertase (cyt-INV) or cell wall invertase (CW-INV).

wound-induced growth will turn out to be an essential factor. We previously reported increased expansion within the growing part of the root and in cotyledons of induced dex-T-*6b* tobacco seedlings (Grémillon *et al.*, 2004). However, roots and cotyledons are difficult to analyze because of their small size and complex organization. Here we demonstrate that *6b* also increases expansion in a simple and reproducible leaf disc expansion system (Keller and Van Volkenburgh, 1997, 1998). Leaf expansion can be stimulated by various factors, including auxins. Jones *et al.* (1998) have used an inducible Arabidopsis auxin-binding protein 1 (*ABP1*) gene to enhance auxin-controlled expansion in tobacco leaf discs. *ABP1* induction in intact plants did not change leaf morphology. Clearly, leaf disc expansion can also be experimentally controlled with an inducible *6b* gene. In contrast to *ABP1*, T-*6b* leads to chlorosis in older leaves and strong morphological changes in young leaves (Grémillon *et al.*, 2004; this paper). It has been reported that *6b* gene expression increases IAA levels (Gális *et al.*, 2002). However, IAA concentrations did not change significantly in dex-induced D6Nt17 leaf discs in spite of increased expansion. Moreover, the IAA-inducible gene *Nt-IAA2.3/2.5* was not induced under these conditions. We therefore conclude that, at least in leaf discs, T-*6b*-induced growth is not accompanied by an increase in IAA. T-*6b*- and IAA-induced expansions were not additive, suggesting that T-*6b* might use part of the IAA-controlled expansion pathway.

Fusicoccin stimulated expansion at concentrations up to 1–2 μM. Even at such FC concentrations, T-*6b* expression still increased expansion and is therefore unlikely to act in the same way as FC, i.e. by cell wall acidification. This is also indicated by the fact that T-*6b* increased leaf osmolality, whereas FC did not. Analysis of 62 metabolites showed that glucose and fructose contributed most to these changes. Although glutamine and proline increased 3.1- and 3.4-fold respectively, they did not significantly change the overall osmolality. Levels of the osmolytically important potassium cation remained constant. Although simultaneous increase in glucose and fructose suggested an increase in invertase activity, measurements on dex-infiltrated leaves showed no such changes. Further metabolic analysis might reveal how the rise in glucose and fructose is brought about. As the 6b protein has been proposed to act on transcription (Kitakura *et al.*, 2002), the changes in glucose and fructose levels may result from transcriptional changes in genes that are involved in osmoregulation or hexose metabolism. Although T-*6b*-induced expansion was most clearly

Table 3 Concentrations of metabolites in mock-induced (control) and dex-induced (plus dex) D6Nt17 leaves

Compound	Control (nmol g^{-1} FW)	Plus dex (nmol g^{-1} FW)	Ratio dex+/dex−
Alanine	342.09 ± 30.7	403.81 ± 43.89	1.2 ± 0.15
Arginine	3.38 ± 0.4	4.98 ± 0.7	1.52 ± 0.26
Asparagine	7.63 ± 1.54	9.53 ± 1.59	1.29 ± 0.26
Aspartate	144.24 ± 41.31	187.71 ± 52.66	1.38 ± 0.46
β-Alanine	9.85 ± 1.52	13.65 ± 2.42	1.42 ± 0.29
Cysteine	139.01 ± 28.2	283.97 ± 62.91	2.13 ± 0.57
γ-Aminobutyric acid	46.57 ± 16.92	32.61 ± 7.41	0.72 ± 0.19
Glutamate	415.18 ± 150.4	567.54 ± 169.2	1.44 ± 0.49
Glutamine	599.09 ± 182.1	1766.85 ± 294.2	**3.12 ± 0.61**
Glycine	131.04 ± 16.68	236.07 ± 28.86	**1.81 ± 0.22**
Isoleucine	4.98 ± 0.36	7.8 ± 0.42	**1.58 ± 0.1**
Leucine	7.47 ± 0.6	9.77 ± 1.48	1.32 ± 0.23
Phenylalanine	18.19 ± 4.82	33.96 ± 2.39	**1.93 ± 0.17**
Proline	13.45 ± 2.91	45.04 ± 8.31	**3.43 ± 0.75**
Serine	267.11 ± 29.65	451.19 ± 126.6	1.77 ± 0.58
Threonine	495.42 ± 62.14	798.47 ± 131.7	1.67 ± 0.34
Valine	42.61 ± 3.37	65.14 ± 5.13	**1.55 ± 0.15**
α-Ketoglutarate	45.39 ± 16.87	65.13 ± 18.22	1.52 ± 0.45
Citramalate	10.65 ± 1.91	17.58 ± 1.55	**1.69 ± 0.15**
Citrate	65.96 ± 12.93	82.97 ± 18.46	1.27 ± 0.29
Dehydroascorbate	843.49 ± 205.9	1045.19 ± 270.9	1.28 ± 0.35
D-isoascorbate	654.12 ± 170.2	1704.65 ± 172.9	**2.7 ± 0.32**
Fumarate	66.97 ± 16.03	122.28 ± 25.22	1.9 ± 0.47
Galacturonate	31.11 ± 5.62	53.68 ± 4.4	**1.78 ± 0.17**
Glycerate	209.2 ± 54.6	296.09 ± 97.67	1.48 ± 0.52
Isocitrate	2.33 ± 0.5	3.02 ± 0.52	1.32 ± 0.25
L-ascorbate	326.91 ± 85.16	852.33 ± 86.45	**2.7 ± 0.32**
Malate	2782.63 ± 522.2	3132.81 ± 427.2	1.86 ± 0.35
Maleate	72.13 ± 13.03	130.81 ± 21.26	1.14 ± 0.16
Shikimate	57.2 ± 3.83	97.99 ± 4.43	**1.73 ± 0.09**
Succinate	62.05 ± 9.34	81.21 ± 9.57	1.33 ± 0.16
Threonate	136.11 ± 27.96	276.49 ± 60.92	2.12 ± 0.56
Arabinose	19.37 ± 1.04	23.21 ± 1.01	**1.21 ± 0.06**
Fructose	4547.94 ± 432.2	14 902.55 ± 393.8	**3.28 ± 0.03**
Galactose	39.28 ± 1.94	34.96 ± 5.32	0.91 ± 0.17
Gentiobiose	4.67 ± 0.53	4.26 ± 0.52	0.92 ± 0.12
Glucose	4278.91 ± 330.1	13 115.88 ± 350.2	**3.06 ± 0.02**
Glycerol	66.52 ± 15.44	53.86 ± 1.43	0.82 ± 0.03
Inositol	1445.29 ± 80.56	1807.13 ± 49.54	**1.26 ± 0.04**
Maltose	25.72 ± 1.49	28.25 ± 0.88	**1.11 ± 0.02**
Mannitol	4.1 ± 0.78	3.63 ± 0.13	0.88 ± 0.04
Mannose	15.31 ± 1.76	23.35 ± 2.15	**1.56 ± 0.18**
Rhamnose	3.87 ± 0.21	3.98 ± 0.13	1.04 ± 0.04
Ribose	10.8 ± 0.7	11.56 ± 0.38	1.08 ± 0.04
Sucrose	4943.29 ± 242.7	7836.93 ± 663.5	**1.58 ± 0.07**
Trehalose	0.99 ± 0.14	1.69 ± 0.17	**1.78 ± 0.19**
Xylose	8.3 ± 0.63	10.56 ± 0.5	**1.29 ± 0.06**
Fructose-6-P	3.59 ± 1.34	4.64 ± 1.76	1.39 ± 0.61
Glucose-6-P	1820.24 ± 722.8	2430.07 ± 919.5	1.43 ± 0.63
Glycerol-1-P	5.94 ± 1.37	8.1 ± 1.86	1.43 ± 0.39
Benzoic acid	67.91 ± 2.76	64.93 ± 3.1	0.96 ± 0.04
C-Caffeic acid	32.95 ± 3.36	35.21 ± 2.26	1.07 ± 0.06
Chlorogenate	779.47 ± 105.7	922.23 ± 51.89	1.22 ± 0.07
Erythritol	9.45 ± 0.22	9.54 ± 0.26	1.01 ± 0.03
Gluconate	93.41 ± 19.34	137.38 ± 7.77	**1.52 ± 0.1**
Glutarate	2.21 ± 0.21	2.44 ± 0.13	1.1 ± 0.05
Nicotinate	2696.12 ± 454.8	2536.43 ± 450.8	0.96 ± 0.19
Putrescine	17.99 ± 2.55	42.34 ± 5.4	**2.4 ± 0.36**

Table 3 (Continued.)

Compound	Control (nmol g^{-1} FW)	Plus dex (nmol g^{-1} FW)	Ratio dex+/dex–
Pyroglutamate	1196.24 ± 112.3	1600.37 ± 66.56	**1.36 ± 0.07**
Saccharic acid	8.62 ± 0.92	10.04 ± 0.69	1.18 ± 0.09
t-Caffeic acid	1.47 ± 0.25	2.18 ± 0.13	**1.52 ± 0.08**
Tyramine	89.76 ± 7.16	89.63 ± 4.1	1.01 ± 0.04

Values are means ± SE. Values in bold are significant differences ($P < 0.05$) as determined by Student's *t*-test.

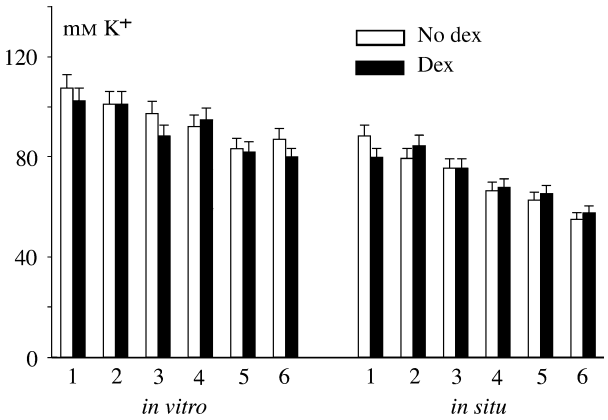

Figure 8. Potassium concentrations in D6Nt17 discs *in vitro* or patches *in situ*.
Leaf discs of six successive leaves (*in vitro*, 1–6, lengths of 17, 18.5, 19, 20.5, 21, 22 cm) were floated on M60 (white bars) or M60D (black bars). Intact leaves (*in situ*, 1–6, lengths of 16.5, 18, 19.5, 20.5, 21.5, 22 cm) were mock-induced (white bars) or dex-induced (black bars) in patches. T-*6b* induction *in vitro* or *in situ* does not lead to significant changes in potassium levels.

observed *in vitro*, limited expansion could also be observed *in situ* at wound areas. The rims of non-induced discs accumulated more glucose, fructose and sucrose than the centre, possibly because of limited transport of sucrose from the medium into the disc. T-*6b* expression enhanced glucose and fructose changes, and particularly high levels accumulated at the rims. We propose that in crown gall formation, the *6b* gene stimulates a local, wound-induced increase in glucose and fructose. The resulting osmolality change would help to prevent desiccation in wound areas (see for example Holmström *et al.*, 1996) and thereby favour cell division under the control of T-DNA-encoded hormone synthesis by the *ipt* and *iaa* genes. At the same time, high glucose and fructose levels may contribute to agrobacterial growth, either directly or after incorporation into opines. So far, only expanding plant organs (roots, hypocotyls, stems, cotyledons, petioles, leaves and wound tissues) have been found to react to *6b* induction, suggesting that *6b* genes cannot initiate the expansion process, but only enhance ongoing expansion. An osmotic role for *6b* genes is consistent with this, as fully expanded tissues will generally not yield to an increase in turgor.

During normal expansion growth of various plant organs, cells must import or synthesize osmolytes to avoid progressive dilution that would otherwise lead to turgor loss. Thus, growth requires a tight control of osmolyte concentrations. In carrots, growing taproots successively use amino acids, ions, hexoses and sucrose as osmolytes (Korolev *et al.*, 2000). How this osmoregulation is achieved is unknown. We have shown that both intact and wounded leaves increase their osmolality upon T-*6b* expression. It seems therefore that T-*6b* can modify the osmotic controls required for normal and wound-induced cell expansion. Further studies with other plant organs such as cotyledons or roots or with plant species other than tobacco will show how general this T-*6b* effect is. It might also be interesting to extend such studies to plants expressing other members of the *plast* family, preferably under inducible promoter control. Some of the pleiotropic *6b* effects might be directly related to the increase in glucose and fructose. Accumulation of hexoses in tobacco leaves leads to bleaching (Jang and Sheen, 1994; Stitt *et al.*, 1990), and this is indeed observed in T-*6b*-expressing leaves and cotyledons (Grémillon *et al.*, 2004; this paper). Accumulation of starch at later stages will also affect photosynthesis and growth.

It remains to be studied whether the remarkable *6b*-induced enation growth effects that occur in non-induced tissues or in grafted wild-type tissues (Grémillon *et al.*, 2004; Helfer *et al.*, 2003; this paper) are also accompanied by osmolyte changes.

Experimental procedures

Leaf disc expansion assays

Leaf disc expansion assays were adapted from Keller and Van Volkenburgh (1997, 1998). Five leaf discs of 1 cm diameter were removed with a cork borer and floated abaxial side up in 3 ml M60 buffer (0.5 mM HEPES, pH 6.0, 10 mM KCl, 60 mM sucrose; in the buffer name, 60 refers to the sucrose concentration in mM). In some cases, the sucrose concentration was varied. After a 30 min equilibration period, FWs were determined. Discs were blotted dry on both sides, rapidly weighed and placed back on the medium. Discs were kept in the dark at 20°C. Fresh weights were measured at regular time intervals and expressed as percentages of the initial FW. Only plants with a height between 20 and 60 cm were used, well before flowering (at about 100 cm). All experiments were repeated at least three times using different plant batches. Experimental errors were <3% (not shown), and expansion of discs from leaf

positions that were symmetrical with respect to the mid-vein differed by <2%.

Two-factor analysis of variance was carried out using MINITAB software (Minitab Inc., State College, PA, USA).

Metabolite profiling and potassium analysis

Comparable, 80% expanded leaves from seven dex-T-*6b* (D6Nt17) plants from the same batch were infiltrated with 10 mM $MgSO_4$ containing 0 or 20 μM dex (one leaf per plant, two patches per leaf side). After 24 h, patches were removed with a cork borer, placed in liquid nitrogen, crushed in a mortar and extracted with MeOH (1 ml MeOH per 65 mg FW), adding 12 μg ribitol per sample as an internal standard. Further extraction and metabolite analyses were done according to Roessner-Tunali *et al.* (2003). Potassium values of intact leaves and leaf discs were determined by atomic emission spectroscopy, using a Varian SPECTRA A20plus (Varian, Palo Alto, CA, USA), at an emission wavelength of 766.5 nm and a slit width of 0.1 nm, using an air-ethylene flame.

Auxin measurements

Several dex-T-6b D6Nt17 plants from the same greenhouse batch were chosen, and from each plant a 80% expanded leaf was selected, from which two symmetrical groups of eight discs were removed. One group was floated on M60 medium, the other on M60D (M60 plus 3 μM dex). Time 0 controls were placed on M60 for 45 min. At 3 h intervals, eight discs from M60 and eight from M60D cultures were blotted dry, weighed, and 1 ml MeOH added per sample. After addition of 14 pmol (^{2}H)2-IAA as an internal standard, discs were extracted for 30 min at 70°C and re-extracted twice with 1.0 and 0.5 ml MeOH. Combined extracts were dried in a SpeedVac (Savant Instruments, Holbrook, NY, USA) and analyzed according to Müller *et al.* (2002). For each time point, 10 samples were measured. Values were analyzed by Student's *t*-test (significant at $P = 0.05$).

Glucose, fructose and sucrose measurements

Glucose, fructose and sucrose were measured with a sequential enzymatic assay, using glucose (G2020), fructose (F2668) and sucrose assay (S1299) kits (all Sigma, Lyon, France).

Gene expression analysis

Auxin-induced gene expression was measured by Northern analysis. Poly(A) RNA was isolated on oligo(dT) cellulose and run on denaturing gels. Purified inserts from *Nt-IAA2.3/2.5* (Dargeviciute *et al.*, 1998; *Not*I–*Xho*I fragment in pBluescript vector), T-*6b* (PCR-amplified T-6b insert from pPM37; Tinland *et al.*, 1989), *NtACT1* (c-DNA, accession number CAA45149.1) and *CaKN*, *NtPCNA* and *NtCYC1* (for references, see Helfer *et al.*, 2003) clones were labelled with ^{32}P-dCTP and hybridized to RNA blots under stringent conditions. Blots were exposed for different times and bands were quantified by ImageJ analysis (Rasband, 1997). Relative band intensities were calculated with respect to the actin standard. Data were analyzed by Student's *t*-test (significant at $P < 0.05$).

Osmolyte measurements

Leaf sap osmolality (expressed in mOsm) was measured as follows: leaf discs were carefully blotted dry, weighed, placed in micro-centrifuge tubes and frozen in liquid nitrogen. After thawing, they were centrifuged at 12 000 ***g*** for 10 min, and 50 μl of the supernatant was placed in a freezing-point osmometer (Osmomat 030; Gonotec, Berlin, Germany). Osmolyte concentrations in leaf tissues were calculated using a dry weight value of 15% FW.

Invertase activities

Activities of cell wall invertases, vacuolar invertases and cytosolic invertases were tested according to Greiner *et al.* (1999). Two discs of 1.6 cm diameter (about 50 mg) from dex- or mock-infiltrated 80% expanded leaves were ground in a mortar on ice, extracted with two volumes of extraction buffer (30 mM MOPS, pH 6.0, 250 mM sorbitol, 10 mM $MgCl_2$, 10 mM KCl, 1 mM PMSF). The extract was centrifuged for 5 min at 12 000 ***g***, and the supernatant incubated with five volumes of 30 mM sodium acetate, pH 4.7, and 30 mM sucrose (for vacuolar invertase), or 50 mM sodium phosphate, pH 7.0, and 30 mM sucrose (for cytosolic invertase). The pellet was washed twice with extraction buffer plus 1% Triton-X100, once with extraction buffer without Triton, and resuspended in 100 μl 30 mM sodium acetate, pH 4.7, 30 mM sucrose (for cell wall invertase). After incubation for 2 h at 37°C on a rotating wheel, vacuolar and cell wall invertase assays were neutralized with 1 M Tris–HCl pH 8.0, and all assays were heated for 3 min at 85°C and centrifuged at 12 000 ***g*** for 10 min. Glucose in the supernatants was measured with the Sigma G2020 glucose assay. In all assays, controls without sucrose were included to measure endogenous glucose levels.

Acknowledgements

We thank our gardeners for greenhouse plants, P. Schall for help with potassium measurements, S. Greiner for help with invertase assays, C. Perrot-Rechenmann for auxin-inducible genes, S. Kauffmann for the actin probe, F. Nobelis for statistical analysis, and E. Van Volkenburgh and A. Fernie for useful discussion.

References

Aducci, P., Marra, M., Fogliano, V. and Fullone, M.R. (1995) Fusicoccin receptors: perception and transduction of the fusicoccin signal. *J. Exp. Bot.* **46**, 1463–1478.

Bateman, A., Coin, L., Durbin, R. *et al.* (2004) The Pfam protein families database. *Nucleic Acids Res.* **32**, D138–D141.

Bonnard, G., Tinland, B., Paulus, F., Szegedi, E. and Otten, L. (1989) Nucleotide sequence, evolutionary origin and biological role of a rearranged cytokinin gene isolated from a wide host range biotype III *Agrobacterium* strain. *Mol. Gen. Genet.* **216**, 428–438.

Dargeviciute, A., Roux, C., Decreux, A., Sitbon, F. and Perrot-Rechenmann, C. (1998) Molecular cloning and expression of the early auxin-responsive Aux/IAA gene family in *Nicotiana tabacum*. *Plant Cell Physiol.* **39**, 993–1002.

Estruch, J.J., Chriqui, D., Grossmann, K., Schell, J. and Spena, A. (1991a) The plant oncogene *rolC* is responsible for the release of cytokinins from glucoside conjugates. *EMBO J.* **10**, 2889–2895.

Estruch, J.J., Schell, J. and Spena, A. (1991b) The protein encoded by the *rolB* plant oncogene hydrolyses indole glucosides. *EMBO J.* **10**, 3125–3128.

Filippini, F., Rossi, V., Marin, O., Trovato, M., Costantino, P., Downey, P.M., lo Sciavo, F. and Terzi, M. (1996) A plant oncogene as a phosphatase. *Nature*, **379**, 499–500.

Gális, I.I., Simek, P., Macas, J., Zahradnickova, H., Vlasak, J., Wabiko, H., Van Dongen, W., Van Onckelen, H.A. and Ondrej, M. (1999) The *Agrobacterium tumefaciens* C58-*6b* gene confers resistance to *N*(6)-benzyladenine without modifying cytokinin metabolism in tobacco seedlings. *Planta*, **209**, 453–461.

Gális, I., Simek, P., Van Onckelen, H., Kakiuchi, Y. and Wabiko, H. (2002) Resistance of transgenic tobacco seedlings expressing the *Agrobacterium tumefaciens* C58-*6b* gene, to growth-inhibitory levels of cytokinin is associated with elevated IAA levels and activation of phenylpropanoid metabolism. *Plant Cell Physiol.* **43**, 939–950.

Greiner, S., Rausch, T., Sonnewald, U. and Herbers, K. (1999) Ectopic expression of a tobacco invertase inhibitor homolog prevents cold-induced sweetening of potato tubers. *Nature Biotechnol.* **17**, 708–711.

Grémillon, L., Helfer, A., Clément, B. and Otten, L. (2004) New plant growth-modifying properties of the *Agrobacterium* T-*6b* oncogene revealed by the use of a dexamethasone-inducible promoter. *Plant J.* **37**, 218–228.

Helfer, A., Pien, S. and Otten, L. (2002) Functional diversity and mutational analysis of *Agrobacterium* 6B oncoproteins. *Mol. Genet. Genomics*, **267**, 577–586.

Helfer, A., Clément, B., Michler, P. and Otten, L. (2003) The *Agrobacterium* oncogene AB-*6b* causes a graft-transmissible enation syndrome in tobacco. *Plant Mol. Biol.* **52**, 483–493.

Holmström, K-O., Mäntylä, E., Welin, B., Mandal, A., Palva, T., Tunnela, O.E. and Londesborough, J. (1996) Drought tolerance in tobacco. *Nature*, **379**, 683–684.

Hooykaas, P.J.J., den Dulk-Ras, H. and Schilperoort, R.A. (1988) The *Agrobacterium tumefaciens* T-DNA gene *6b* is an onc gene. *Plant Mol. Biol.* **11**, 791–794.

Jang, J.C. and Sheen, J. (1994) Sugar sensing in higher plants. *Plant Cell*, **6**, 1665–1679.

Jones, A.M., Im, K-H., Savka, M.A., Wu, M-J., DeWitt, N.G., Shillito, R. and Binns, A. (1998) Auxin-dependent cell expansion mediated by overexpressed auxin-binding protein 1. *Science*, **282**, 1114–1117.

Keller, C.P. and Van Volkenburgh, E. (1997) Auxin-induced epinasty of tobacco leaf tissues. *Plant Physiol.* **113**, 603–610.

Keller, C.P. and Van Volkenburgh, E. (1998) Evidence that auxin-induced growth of tobacco leaf tissues does not involve cell wall acidification. *Plant Physiol.* **118**, 557–564.

Kitakura, S., Fujita, T., Ueno, Y., Terakura, S., Wabiko, H. and Machida, Y. (2002) The protein encoded by the oncogene *6b* from *Agrobacterium tumefaciens* interacts with a nuclear protein of tobacco. *Plant Cell*, **14**, 451–463.

Korolev, A.V., Deri Tomos, A., Bowtell, R. and Farrar, J.F. (2000) Spatial and temporal distributions of solutes in the developing carrot taproot measured at single-cell resolution. *J. Exp. Bot.* **51**, 567–577.

Levesque, H., Delepelaire, P., Rouzé, P., Slightom, J. and Tepfer, D. (1988) Common evolutionary origin of the central portion of the Ri TL-DNA of *Agrobacterium rhizogenes* and the Ti T-DNAs of *Agrobacterium tumefaciens*. *Plant Mol. Biol.* **11**, 731–744.

Meyer, A., Tempé, J. and Costantino, P. (2000) Hairy root: a molecular overview. Functional analysis of *Agrobacterium rhizogenes* T-DNA genes. In *Plant–Microbe Interactions*, Vol. 5 (Stacey, G. and Keen, N.T., eds). St Paul, Minnesota: APS Press, pp. 93–139.

Müller, A., Düchting, P. and Weiler, E.W. (2002) A multiplex GC–MS/MS technique for the sensitive and quantitative single-run analysis of acidic phytohormones and related compounds, and its application to *Arabidopsis thaliana*. *Planta*, **216**, 44–56.

Nilsson, O. and Olsson, O. (1997) Getting to the root: the role of the *Agrobacterium rhizogenes rol* genes in the formation of hairy roots. *Physiol Plant.* **100**, 463–473.

Otten, L. and Helfer, A. (2001) Biological activity of the *rolB*-like 5′ end of the A4 *orf8* gene from the *Agrobacterium rhizogenes* TL-DNA. *Mol. Plant–Microbe Interact.* **14**, 405–411.

Rasband, W.S. (1997) ImageJ, U.S. National Institutes of Health, Bethesda, MA, USA. http://rsb.info.nih.gov/ij/

Roessner-Tunali, U., Hegemann, B., Lytovchenko, A., Carrari, F., Bruedigam, C., Granot, D. and Fernie, A.R. (2003) Metabolic profiling of transgenic tomato plants overexpressing hexokinase reveals that the influence of hexose phosphorylation diminishes during fruit development. *Plant Physiol.* **133**, 84–99.

Spanier, K., Schell, J. and Schreier, P.H. (1989) A functional analysis of T-DNA gene *6b*: the fine tuning of cytokinin effects on shoot development. *Mol. Gen. Genet.* **219**, 209–216.

Stieger, P.A., Meyer, A.D., Kathmann, P., Fründt, C., Niederhauser, I., Barone, M. and Kuhlemeier, C. (2004) The *orf13* T-DNA gene of *Agrobacterium rhizogenes* confers meristematic competence to differentiated cells. *Plant Physiol.* **135**, 1798–1808.

Stiles, K.A., McClintick, A. and Van Volkenburgh, E. (2003) A developmental gradient in the mechanism of K^+ uptake during light-stimulated leaf growth in *Nicotiana tabacum* L. *Planta*, **217**, 587–596.

Stitt, M., Von Schaewen, A. and Willmitzer, L. (1990) 'Sink' regulation of photosynthetic metabolism in transgenic tobacco plants expressing yeast invertase in their cell wall involves a decrease in the Calvin-cycle enzymes and an increase of glycolytic enzymes. *Planta*, **183**, 40–50.

Tinland, B., Huss, B., Paulus, F., Bonnard, G. and Otten, L. (1989) *Agrobacterium tumefaciens 6b* genes are strain-specific and affect the activity of auxin as well as cytokinin genes. *Mol. Gen. Genet.* **219**, 217–224.

Tinland, B., Rohfritsch, O., Michler, P. and Otten, L. (1990) *Agrobacterium tumefaciens* T-DNA gene *6b* stimulates *rol*-induced root formation, permits growth at high auxin concentrations and increases root size. *Mol. Gen. Genet.* **223**, 1–10.

Tinland, B., Fournier, P., Heckel, T. and Otten, L. (1992) Expression of a chimeric heat-shock inducible *Agrobacterium 6b* oncogene in *Nicotiana rustica*. *Plant Mol. Biol.* **18**, 921–930.

Umber, M., Voll, L., Weber, A., Michler, P. and Otten, L. (2002) The *rolB*-like part of the *Agrobacterium rhizogenes orf8* gene inhibits sucrose export in tobacco. *Mol. Plant–Microbe Interact.* **15**, 956–962.

Umber, M., Clément, B. and Otten, L. (2005) The T-DNA oncogene A4-*orf8* from *Agrobacterium rhizogenes* strain A4 induces abnormal growth in tobacco. *Mol. Plant–Microbe Interact.* **18**, 205–211.

Wabiko, H. and Minemura, M. (1996) Exogenous phytohormone-independent growth and regeneration of tobacco plants transgenic for the *6b* gene of *Agrobacterium tumefaciens* AKE10. *Plant Physiol.* **112**, 939–951.

Würtele, M., Jelich-Ottmann, C., Wittinghofer, A. and Oecking, C. (2003) Structural view of a fungal toxin acting on a 14-3-3 regulatory complex. *EMBO J.* **22**, 987–994.